JOURNAL OF OPTOELECTRONICS AND ADVANCED MATERIALS Vol. 9, No. 12, December 2007, p. 3743 - 3746

Structural and morphological properties of thermally evaporated $Zn_{1-x}Mn_xS$ nanocrystalline films

D. SREEKANTHA REDDY[*, a], M. MAHESWARA REDDY[b], K. NARASIMHA RAO[a], K. R. GUNASEKHAR[a], P. SREEDHARA REDDY[b]

[a] *Department of Instrumentation, Indian Institute of Science, Bangalore-560012, India*

[b] *Department of Physics, Sri Venkateswara University, Tirupati-517502, India*

In recent years the dilute magnetic semiconductors have received much attention due to the complementary properties of semiconductor and ferromagnetic behaviour. Nanostructured $Zn_{1-x}Mn_xS$ films ($0 \le x \le 0.25$) were deposited on glass substrates at room temperature (300 K) using simple resistive thermal evaporation technique. All the deposited films were characterized by chemical, structural and morphological studies. Scanning Electron Microscopy (SEM) and Atomic Force Microscopy (AFM) studies showed that all the films investigated were in nanocrystalline form with the grain size lying in the range 8 – 22 nm. All the films exhibited cubic structure and the lattice parameter varied linearly with composition.

(Received August 19, 2007; accepted December 5, 2007)

Keywards: Diluted Magnetic Semiconductors (DMS), Thermal evaporation technique, $Zn_{1-x}Mn_xS$ Nanocrystalline films, Morphological studies, Structural studies

1. Introduction

Diluted magnetic semiconductors (DMS) are semiconductors doped with magnetic impurities and combine therefore magnetic with semiconducting properties. For this reason they appear to represent a new type of materials for spintronics, whose Curie temperature, however, for practical applications has to be (well) above room temperature. Semiconducting and magnetic properties of $A^{II}_{1-x}Mn_xB^{VI}$ materials (II= Zn, Cd, Hg, VI= S, Se, Te) are investigated. Emphasis is put on the studies of exchange interaction between magnetic ions in the wide-gap semiconductors like $Zn_{1-x}Mn_xTe$, and between free carriers and magnetic ions in the narrow-gap materials as $Hg_{1-x}Mn_xTe$ and $Hg_{1-x}Mn_xSe$. Doped semiconductors have attracted extensive research interests in the recent years due to their unique optical and potential applications [1, 2]. Diluted magnetic semiconductors (DMS) are expected to play an important role in interdisciplinary materials science and future electronics because charge and spin degrees of freedom accommodated into a single material exhibits interesting magnetic, magneto-optical, magnetoelectronic and other properties [3]. Within the next few years, it is expected that magnetoelectronic chips will be used in quantum computers. An inherent advantage of magnetoelectronics over electronics is the fact that magnet tend to stay magnetized for long. Hence this arises interest in industries to replace the semiconductor-based components of computer with magnetic ones, starting from RAM. The new magnetic RAM will retain data even when the computer is turned off. And most important advantage will be eliminating the time consuming process of 'booting up' information from hard drive to processor like a TV set, all the information would be there. Most importantly, state of magnetization changes the electronic properties and vice versa through the spin exchange interaction between local magnetic moments and carriers. The wide variety of both host crystals and magnetic atoms provides materials which range from wide gap to zero gap semiconductors, and which reveal many different types of magnetic interaction. Several of the properties of these materials may be tuned by changing the concentrations of the magnetic ions.

2. Experimental procedure

$Zn_{1-x}Mn_xS$ nanocrystalline films were prepared at various compositions (x = 0.0, 0.05, 0.1, 0.15, 0.2 and 0.25) by thermal evaporation technique. The films were grown on glass substrates at room temperature (300 K). Appropriate quantities of 5N pure ZnS and MnS powders (Sigma Aldrich, Germany) were thoroughly mixed by grinding them with pestle and mortar. Direct evaporation of the mixture in powder form resulted in spattering of the powder when the boat is heated. Hence, the mixtures were made into pellets using hydraulic press with 2 MPa. Only in pellet form it was possible to evaporate the material completely. The source to substrate distance was maintained at ≈15 cm to get a deposition rate of ~15 Å/s. Every time, known fixed quantity of material was loaded in the boat and was completely evaporated. The thicknesses of the films were ~ 0.4 μm. The depositions were carried out in a high vacuum system having diffusion pump backed by rotary pump and with liquid nitrogen trap. Coatings were carried out in the pressure range of 2×10^{-6} m bar. The thickness of the films was monitored using a quartz crystal thickness monitor (Model QTM101).

The as-deposited $Zn_{1-x}Mn_xS$ films were subjected to various characterization studies. The composition of the films was estimated using Energy Dispersive Analysis of

X-rays (EDAX; Serion) attached to Field Emission Scanning Electron Microscope (FE - SEM). The grain size and root mean square (rms) surface roughness of the films were obtained by Atomic Force Microscopy (AFM, Model: Veeco CP 2). The structure of the films was studied using X-ray diffractometer (XRD, Model: Phillip's X'Pert Pro) in the scanning range of $2\theta = 20 - 70^0$.

3. Results and discussions

The deposited $Zn_{1-x}Mn_xS$ nanostructured films were high transparent, pinhole free and strongly adherent to the surface of the substrate.

3.1. Composition and structural analysis

Manganese is different from other transition metals when substituted in an $A^{II}B^{VI}$ matrix, since it forms stable phases over a wide range of compositions. It appears that the ease with which the manganese substitutes for the group II elements in the zinc blende and wurtzite structures results from the fact that the 3d orbital of Mn are exactly half-filled. In fact that high solubility of manganese is remarkable for all $A^{II}_{1-x}Mn_xB^{VI}$ solid solutions [4]. Typical EDAX spectra were shown in Fig. 1. Chemical compositions of the constituents obtained from EDAX deviated from the target compositions within ± 0.02 at. % which is very small. Hence in all the future discussions only the target compositions will be used.

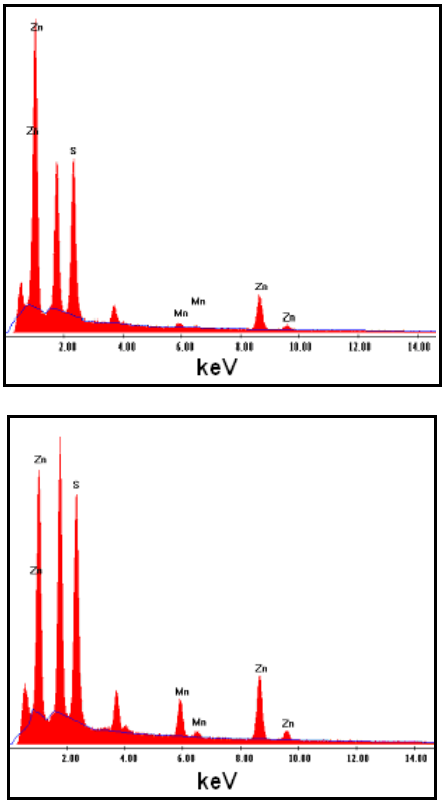

Fig. 1. Typical EDAX spectra of $Zn_{0.95}Mn_{0.05}S$ and $Zn_{0.75}Mn_{0.25}S$ nanocrystalline films deposited at 300 K.

X-ray diffraction (XRD) patterns were recorded using a Phillip's X'Pert Pro with Cu K_α radiation (1.5405 Å) as the x-ray source. The representative XRD patterns of Zn1-xMnxS nanostructured films are shown in Fig. 2 as a function of 2θ. All nanostructured films showed similar XRD patterns. The significant peak intensity and line broadening observed in the XRD patterns were attributed to both particle size and crystal defects. That indicates that $Zn_{1-x}Mn_xS$ retains the crystal structure of "parent" ZnS. Pure ZnS films grown at room temperature exhibited a dominant peak at $2\theta = 28.63^0$ which corresponds to (111) plane. When viewed with computer software along with this a small peak at 47.46^0 diffracted along (220) plane is also observed.

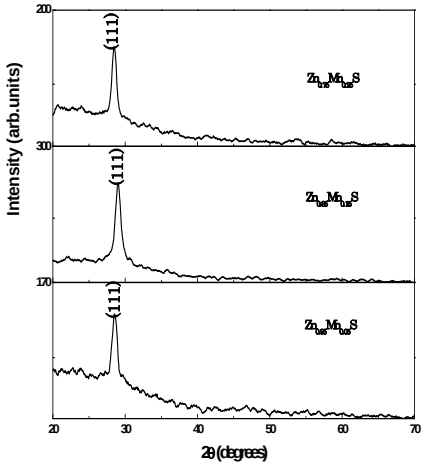

Fig. 2. Comparative XRD spectra of nanostructured pure $Zn_{0.95}Mn_{0.05}S$, $Zn_{0.85}Mn_{0.15}S$ and $Zn_{0.75}Mn_{0.25}S$ films deposited at 300 K.

The position of (111) peak shifted towards lower diffraction angles with the increase of Mn content in the layers, indicating the presence of tensile strain in the grown films. The XRD patterns agree with that of the zinc-blende modification of ZnS. The calculations based on Scherrer formula [5] showed the average crystallite diameters of nanostructured films were approximately 8 – 22 nm. Similar variation in grain size was also observed in AFM and SEM studies.

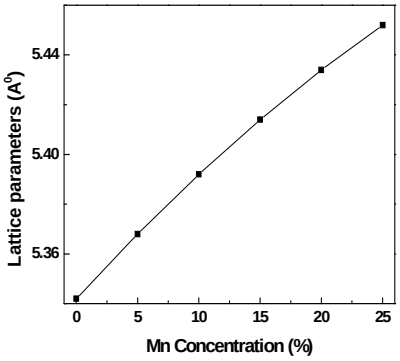

Fig. 3. Variation of lattice parameter with Mn concentration of $Zn_{1-x}Mn_xS$ films.

An obvious change in the lattice parameters of $Zn_{1-x}Mn_xS$ films is observed with increase in Mn content. The lattice parameters 'a' calculated from the XRD data and are shown in Fig. 3. The lattice parameters increased linearly with increasing 'x', following Vegard's law. This confirms the formation of substitutional alloys of $Zn_{1-x}Mn_xS$. Earlier workers [6] reported cubic structure of $Zn_{1-x}Mn_xS$ nanocrystals were prepared colloidal chemistry procedure in the composition range x = 0 – 2% and by aqueous solution precipitation method [7] in the composition range x = 0 – 5%. Substitution of Mn^{2+} (ionic radius 0.8 Å) for Zn^{2+} (ionic radius 0.74 Å) requires a local expansion of the lattice to accommodate the manganese ion. This induces a higher covalent bonding for the Mn^{2+} substitutes in $Zn_{1-x}Mn_xS$ than in other alloys where the incorporation of Mn leads to a local contraction of the lattice (as in the case of Cd compounds).

The lattice parameters of all DMS ternary alloys obey Vegard's law very closely [8]. The same holds for $Zn_{1-x}Mn_xS$, since the 'a' lattice parameters deduced from XRD θ – 2θ scan show a monotonous increase with Mn concentration [9]. Lu et al [10] also reported similar structure of $Zn_{1-x}Mn_xS$ nanocrystals prepared by chemical precipitation method at room temperature. Since in the ideal case lattice parameter 'a' is determined by the nearest neighbor distance 'd' of the anion (or cation) sublattice, one can conclude that 'd' is one of the key parameter, which determines the structural dimensions of the ternary DMS alloy. The dependence of the a lattice parameter on the Mn concentration actually mirrors the evolution of the distance d_c between nearest like atoms, regardless of the structure, so that Vegard's law can be presented in a unified picture for the entire $A^{II}_{1-x}Mn_xB^{VI}$ family, wurtzite and zinc-blende alike. A natural upper limit on the Mn mole fraction x in $A^{II}_{1-x}Mn_xB^{VI}$ crystals is imposed by the fact that MnB^{VI} binary compounds do not naturally crystallize in the zinc blende or wurtzite structures.

3.2. Surface topology and morphology studies

The surface topology of the $Zn_{1-x}Mn_xS$ films carried out by SEM reveals appreciable difference between pure ZnS and Mn-doped ZnS films. All the as-deposited films of all compositions had a small granular surface structure. This indicates the increase in crystallanity of the films on Mn concentration.

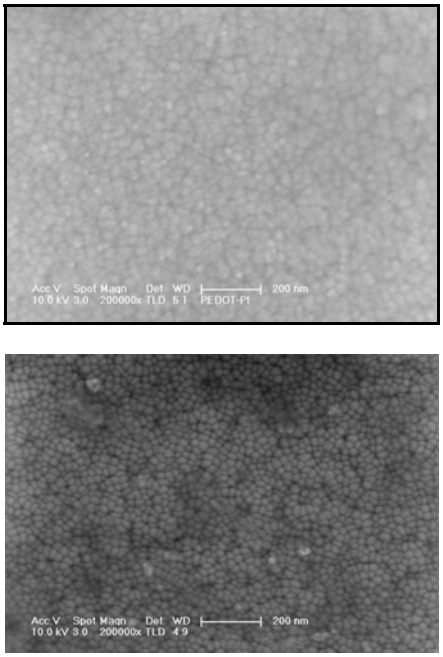

Fig. 4. Typical SEM photograph of $Cd_{0.95}Mn_{0.05}S$ and $Cd_{0.75}Mn_{0.25}S$ films deposited at 300 K.

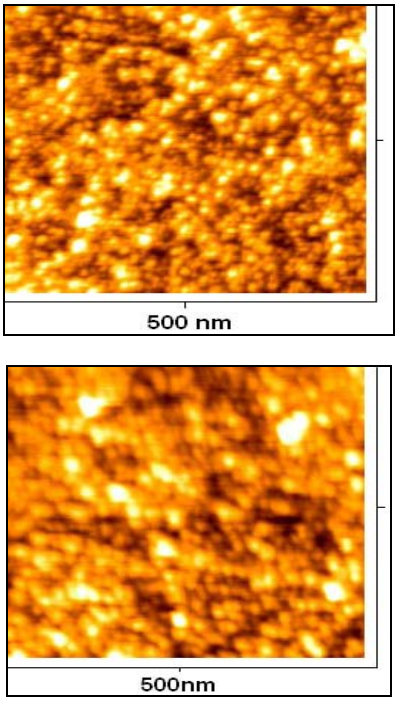

Fig. 5. AFM images of nanostructured (a) $Zn_{0.95}Mn_{0.05}S$ and (b) $Zn_{0.75}Mn_{0.25}S$ films deposited at 300 K.

The SEM micrographs are shown in Fig. 4. The surface morphology of all the as-deposited $Zn_{1-x}Mn_xS$ nanostructured films was studied using AFM. The typical AFM pictures for two concentrations x =0.05 & 0.15 are shown in Fig. 5. The surface morphology of $Zn_{1-x}Mn_xS$ films changes with increase in Mn concentration. The

crystallite size (8 - 22 nm) evaluated from this study is comparable with the data obtained from XRD studies. It is observed that the films of lower 'x' exhibited shallow voids in between the grains. The number of voids on the surface of the films decreased with increased in 'x'.

4. Conclusions

$Zn_{1-x}Mn_xS$ ($0 \leq x \leq 0.25$) nanostructured films were prepared at room temperature (300 K) by simple inexpensive resistive thermal evaporation technique. All the films exhibited cubic structure and crystallite size varied from 8 - 22 nm. The lattice parameter increased linearly with increasing 'x', following Vegard's law. This confirms the formation of substitutional alloys of $Zn_{1-x}Mn_xS$. These materials are used in spintronics and optoelectronic device applications.

References

[1] R. N. Bhargava, D. Gallagher, T. Welker, J. Lumin. **60** and **61**, 275 (1994).
[2] R. N. Bhargava, D. Gallagher, X. Hong, A. Nurmikko, Phys. Rev. Lett. **72**, 416 (1994).
[3] T. Mizokawa, T. Namba, A. Fujimori, T. Fukumura and M. Kawasaki Phys. Rev. B**65,** 085209 (2002).
[4] J. K. Furdyna, J. Appl. Phys. **64,** R 29 (1988).
[5] P. Scherrer, Go¨ttinger Nachrichten. **2,** 98 (1990).
[6] J. Qi, X. Guo, K. Sakurai, Y. Masumoto, Scripta mater. **44**, 2315 (2001).
[7] Balram Tripathi, Y. K. Vijay, Sanjay Wate, F. Singh, D. K. Avasthi, Solid-State Electronics **51**, 81 (2007).
[8] J. K. Furdyna, J. Kossut, Semiconductors and Semimetals, vol. **25**, Academic Press, p. 470 (1988).
[9] E. Chikoidze, Y. Dumont, F. Jomard, J. Appl. Phys. **97,** D327 (2005).
[10] Song Wei Lu, Gurtrand I. Lee, Zhong Lin Wang, Wusheng Tong, Brent K. Wagner Park and Christopher J. Summers; J. Lumin. **91**, 73 (2001).

*Corresponding author: dsreddy_physics@rediffmail.com